

1 **Process modeling and control applied to real-time monitoring of distillation** 2 **processes by near-infrared spectroscopy**

3 Rodrigo R. de Oliveira^{1,2}, Ricardo H. P. Pedroza², Adriano O. Sousa², Kássio M. G.
4 Lima^{2,3}, Anna de Juan^{1*}

5 ¹Chemometrics Group, Department of Analytical Chemistry, Universitat de Barcelona, Diagonal 645,
6 08028, Barcelona, Spain

7 ²LabPVT, Federal University of Rio Grande do Norte, Av. Senador Salgado Filho, 3000, Natal 59078-
8 970, RN, Brazil

9 ³Institute of Chemistry, Biological Chemistry and Chemometrics, Federal University of Rio Grande do
10 Norte, Av. Senador Salgado Filho, 3000, Natal 59078-970, RN, Brazil

11 *Corresponding author. Tel.: +34 934 03 9778.

12 e-mail address: anna.dejuan@ub.edu (A. de Juan).

13
14 **Abstract:** A distillation device that acquires continuous and synchronized measurements of
15 temperature, percentage of distilled fraction and NIR spectra has been designed for real-time
16 monitoring of distillation processes. As a process model, synthetic commercial gasoline
17 batches produced in Brazil, which contain mixtures of pure gasoline blended with ethanol
18 have been analyzed. The information provided by this device, i.e., distillation curves and NIR
19 spectra, has served as initial information for the proposal of new strategies of process
20 modeling and multivariate statistical process control (MSPC). Process modeling based on
21 PCA batch analysis provided global distillation trajectories, whereas multiset MCR-ALS
22 analysis is proposed to obtain a component-wise characterization of the distillation evolution
23 and distilled fractions. Distillation curves, NIR spectra or compressed NIR information under
24 the form of PCA scores and MCR-ALS concentration profiles were tested as the seed
25 information to build MSPC models. New on-line PCA-based MSPC approaches, some
26 inspired on local rank exploratory methods for process analysis, are proposed and work as
27 follows: a)MSPC based on individual process observation models, where multiple local PCA
28 models are built considering the sole information in each observation point; b) Fixed Size
29 Moving Window – MSPC, in which local PCA models are built considering a moving
30 window of the current and few past observation points; and c) Evolving MSPC, where local
31 PCA models are built with an increasing window of observations covering all points since the

32 beginning of the process until the current observation. Performance of different approaches
33 has been assessed in terms of sensitivity to fault detection and number of false alarms. The
34 outcome of this work will be of general use to define strategies for on-line process monitoring
35 and control and, in a more specific way, to improve quality control of petroleum derived fuels
36 and other substances submitted to automatic distillation processes monitored by NIRS.

37 **Keywords:** Near-infrared spectroscopy; on-line multivariate statistical process control
38 - MSPC; process modeling; distillation process; petroleum.

39

40 **1. Introduction**

41 Distillation curves are frequently used for quality control of petroleum products. The
42 evolution and shape of these curves is directly related to the composition and chemical
43 characteristics of these products and, hence, a temperature deviation from normal distillation
44 behavior may be an indicator of adulteration. ASTM D86 [1] is the standard test method
45 required to obtain distillation curves and classical process control is made by comparing the
46 temperature at specific distillation points with standard specification limits.

47 However, distillation curves, based only on boiling temperature monitoring, are not
48 conclusive to identify adulterations in product composition. Adulterants can nowadays be
49 chosen so that the modified petroleum products show normal distillation curve behavior.
50 Near-infrared spectroscopy (NIRS) may help to overcome such scenario because of the rich
51 physicochemical information associated with this spectroscopic technique and the existence
52 of many NIR sensors designed for on-line process monitoring. Along this line, distillation
53 devices that incorporate NIR sensors and collect synchronized distillation temperatures and
54 related NIR absorption spectra measurements, as proposed by Pasquini and Scafi, are a
55 suitable solution [2]. Thus, the fiber optic probes coupled to NIR spectrometers can be located
56 directly in the distillation process stream, allowing continuous real-time in-process
57 measurements [2–4]. Therefore, information representing both physical and chemical
58 properties of the distilled sample can be derived from each distillation batch.

59 In Brazil, commercial gasoline is blended with ethanol. Thus, gasoline derived
60 directly from refineries without ethanol addition is denominated “type A”. Gasoline “type C”
61 is the commercial mixture of gasoline “type A” and $(27 \pm 1)\%$ of ethanol (% v/v) [5]. As a
62 process model for this work, a study of quality control of Brazilian gasolines regarding
63 ethanol content specification is proposed. To do the experimental process monitoring, an
64 improved version of the automatic distillation device monitored by NIRS proposed by
65 Pasquini and Scafi [2], which allows continuous and synchronized data acquisition and
66 storage of distillation temperatures, distilled mass and related NIR spectra, is proposed.
67 Detailed description of the experimental setup is found in section 2 below.

68 The distillation curves and NIR spectra collected from distillation batch processes can
69 be modelled with principal component analysis (PCA) [6] and multivariate curve resolution –
70 alternating least squares (MCR-ALS) [7] for better process understanding and use of this
71 information in further process control. PCA batch analysis provides global distillation

72 trajectories, whereas MCR-ALS offers the additional value of describing the temperature-
73 dependent evolution and characterization of the different distilled fractions during the process.

74 MSPC has been used to control processes related to very diverse fields, such as
75 pharmacy [8–11], petrochemistry [12–14] and biotechnology [15,16]. Batch MSPC using
76 NIRS has been described in recent works [3,4,8–11,16,17]; however, no MSPC using NIRS
77 to monitor batch distillation process has been reported in the literature.

78 In this study, different off-line process control models are studied using complete
79 batch information collected during the distillation process monitored by NIRS. Distillation
80 curves, original NIR spectra, as well as the compressed spectral information contained in
81 PCA scores or MCR-ALS concentration profiles are used to build off-line PCA-based
82 multivariate statistical process control (MSPC) models. To our knowledge, there is no report
83 in the literature about using the concentration profiles from MCR-ALS analysis as starting
84 information to build PCA-based MSPC models. In this framework, the description of the
85 separate components of the process provided by MCR-ALS would allow for using all
86 concentration profiles on the MSPC model or profiles of selected compounds that could be
87 envisioned as more specific indicators of process evolution.

88 NIR measurements obtained from distillation processes are also used to build on-line
89 batch MSPC models. On-line batch MSPC approaches commonly used are based on the
90 methods proposed by Nomikos and MacGregor [18–20] and Wold et. al. [21]. Other
91 approaches are proposed by Rännar et. al. for adaptive batch monitoring using hierarchical
92 PCA [22], by Zhao et. al using multiple PCA models for local model building at each
93 observation point [23] and using moving window [24]. In this work, chemometric tools
94 typically used to perform local exploratory analysis of the evolution of processes, such as
95 evolving factor analysis (EFA) or fixed size moving window - EFA (FSMW-EFA) [25,26],
96 have been adopted to propose new on-line batch MSPC strategies. The performance of these
97 on-line MSPC approaches has been studied in terms of sensitivity to fault detection and
98 number of false alarms.

99 The outcomes of this study will be of general applicability, as guidelines for process
100 modeling and control based on spectroscopic measurements, and suppose a significant
101 improvement on the specific field of quality control based on distillation processes, both from
102 the instrumental point of view and from the way to handle the derived information from
103 coupled temperature-NIR distillation curves.

104 2. Experimental

105 2.1. Automatic distillation device setup

106 The automatic distillation device designed is shown in Figure 1. It is formed by a
107 distillation glassware setup (125 ml), a transmittance flow cell connected through optical
108 fibers to a FT-NIR spectrophotometer (Rocket, ARCOptix ANIR, Switzerland), an analytical
109 balance (XS204, Mettler-Toledo, Switzerland), a thermocouple and heater controlled by a
110 data acquisition device and a personal computer with a data acquisition software that connects
111 and controls the distillation setup. Heating mantle power applied is automatically controlled
112 based on a feedback controller to keep distillation rate constant rather than keeping constant
113 power as in [2].

114 **(Insert Figure 1)**

115 2.1. Batch distillation process

116 For every distillation batch, 100 mL from the suitable sample, previously weighed, are
117 introduced in the distillation flask. The heater is started and once the initial boiling point
118 (IBP) is automatically detected, distillation process starts and synchronized measurements of
119 temperature, distillation recovered percentage (wt%) of initial sample weight and NIR
120 absorption spectra (900 – 2600 nm) are taken every five seconds until the end point (EP) is
121 reached. Data are stored in MATLAB format in such a way that values every 1 wt% are
122 saved. Temperature and NIR spectra are averages of all measurements recorded during every
123 1 wt% distillation interval.

124 Synthetic gasoline (type C) batches were distilled using the designed automatic
125 distillation device. The gasoline batches were prepared by mixing ethanol AR (99% Sigma-
126 Aldrich) and pure gasoline (type A, from Petrobras refinery) at different ratios. A set of 23
127 blends was performed: 11 samples containing 27 %(v/v) ethanol (on-specification gasolines)
128 and 12 with 10-25 %(v/v) and 30-40 %(v/v) ethanol (off-specification gasolines). Table 1
129 describes the gasoline batches prepared with their related composition. These batch ID labels
130 will be used to identify the batches throughout the manuscript.

131 **(Insert Table 1)**

132 **3. Data treatment**

133 **3.1. Raw data and preprocessing**

134 Temperature, distilled weight and NIR spectra were obtained synchronously every 5 s
135 and averaged measures were stored every 1 wt% of distilled weight increment from IBP until
136 EP. The final process range considered was from 5 to 90 wt% distilled weight, which
137 corresponded to $K = 86$ observation points. Observations at the beginning (< 5 wt%) and end
138 (> 90 wt%) of the distillation process were unstable and, therefore, not used for process
139 control. NIR spectra working wavelength range was 1103 – 2228 nm due to high noise
140 observed in measurements out of these wavelength boundaries. This range contained $J = 573$
141 spectral channels. For each distillation batch, a column-vector sized ($K \times 1$) with the
142 temperatures associated with the distillation curve and a matrix sized ($K \times J$) with the related
143 NIR infrared spectra were obtained.

144 Data obtained from on-specification batch B07 are used to illustrate the typical data
145 obtained at the end of a batch distillation run. Figure 2(a) shows the distillation curve with the
146 recorded boiling temperatures, Figure 2(b) the related raw NIR spectra and Figure 2(c) the
147 raw NIR spectra at the four observation points indicated in Figure 2(a).

148 **(Insert Figure 2)**

149 NIR spectra were preprocessed for baseline correction by Savitzky-Golay derivative
150 [27] (1st order derivative, 2nd order polynomial function and 9 points window) followed by
151 signal intensity fluctuation corrected by spectral normalization, see Figure 3(b).

152 **(Insert Figure 3)**

153 **3.2. Data analysis**

154 **Process modeling. Principal Component Analysis (PCA) and Multivariate Curve**
155 **Resolution-Alternating Least Squares (MCR-ALS).**

156 The matrices with the NIR data from each on-specification batch were arranged one
157 on top of each other into a column-wise augmented multiset structure, **D**, and modeled using
158 principal component analysis (PCA) and multivariate curve resolution-alternating least
159 squares (MCR-ALS). PCA provided a global model of trajectories explaining the overall
160 process evolution, whereas MCR-ALS provided a model describing the evolution and

161 chemical identity of each component (distinct distilled fraction) in the distillation batches
162 analyzed.

163 PCA was used to reduce the dimensionality of the spectral data from the distillation
164 processes by compressing the high-dimensional mean-centered original NIR data matrix into
165 a low-dimensional subspace of principal components. These components explain most of the
166 data variability and are orthogonal linear combinations of the original spectroscopic variables
167 [6]. The PCA model of column-wise augmented matrix \mathbf{D} is expressed as: $\mathbf{D} = \mathbf{TP}^T$, where \mathbf{T}
168 are the scores, related to the observations of the distillation process and \mathbf{P}^T are the loadings,
169 related to the importance of the NIR wavelengths in the description of the principal
170 components. The scatter plot of scores provides the global trajectories of the processes
171 analyzed.

172 The same multiset structure was modeled using multivariate curve resolution -
173 alternating least squares (MCR-ALS). MCR-ALS assumes a bilinear model, $\mathbf{D} = \mathbf{CS}^T$, which
174 is the multiwavelength extension of the Lambert-Beer's law [7,28–30]. \mathbf{S}^T contains the pure
175 spectra of the components needed to describe the distillation process and \mathbf{C} the concentration
176 (distillation profiles). In contrast to PCA, MCR-ALS gives real meaningful concentration and
177 spectral profiles of pure components of the system. MCR-ALS works by alternatingly
178 optimizing \mathbf{C} and \mathbf{S}^T under constraints. Initial estimates of \mathbf{S}^T were performed by using a pure
179 variable selection method based on SIMPLISMA [31]. Constraints applied in this work were
180 non-negativity and unimodality, i.e., presence of a single maximum per profile, for the
181 concentration (\mathbf{C}) profiles. Local rank constraints, i.e., setting the absence of certain
182 compounds in observations of the concentration profiles, were used to improve the quality of
183 the resolved spectral signatures [32]. This was done by appending pure ethanol NIR spectra to
184 the column-wise multibatch structure (in this case, only the ethanol was set to be present in
185 the concentration elements linked to the appended pure ethanol spectra).

186 MCR-ALS provides a much more detailed description of the process than PCA in
187 terms of characterization of process profiles and spectral signatures, related to distillation
188 fractions in this case. However, the single process trajectory provided by the scatter score plot
189 of PCA is a global description of process evolution and a quick visual way to observe when a
190 batch process evolves as NOC batches or does differently. Being complementary views about
191 the evolution of a process, we found relevant to include both in this study. Both PCA scores

192 and MCR **C** profiles are afterwards used as starting information for off-line batch MSPC
 193 models described in the next section.

194 **Process control**

195 From the batches analyzed, nine on-specifications or NOC (Normal Operation
 196 Conditions) batches (batches B01-09), were selected to build PCA-based MSPC models (see
 197 Table 1). These models were afterwards used to detect whether a new batch (or observations
 198 within it) is in or out of control [33]. Two on-specification batches (B10-11) and twelve off-
 199 specification batches (B12-23) were used to test the MSPC models.

200 The PCA-based MSPC model is built using the preprocessed and mean-centered data
 201 matrix of NOC batches, \mathbf{X}_{NOC} , sized (nr. of NOC batches \times observed measurements per batch)
 202 according to the equation below,

$$\mathbf{X}_{\text{NOC}} = \mathbf{T}_{\text{NOC}}\mathbf{P}_{\text{NOC}}^T + \mathbf{E}_{\text{NOC}} \quad (1)$$

203 where \mathbf{T}_{NOC} is the scores matrix of all NOC batches and $\mathbf{P}_{\text{NOC}}^T$ is the loadings matrix. The
 204 number of components used in an MSPC model is a critical parameter and has been
 205 established by cross-validation [34].

206 The scores for new batches are obtained multiplying the measured preprocessed batch
 207 information, \mathbf{X}_{NEW} , with the loadings matrix $\mathbf{P}_{\text{NOC}}^T$ from the model built with the NOC
 208 batches, using the following equation:

$$\mathbf{T}_{\text{NEW}} = \mathbf{X}_{\text{NEW}}\mathbf{P}_{\text{NOC}} \quad (2)$$

209 Then, the residuals are obtained using the new batch scores, as:

$$\mathbf{E}_{\text{NEW}} = \mathbf{X}_{\text{NEW}} - \mathbf{T}_{\text{NEW}}\mathbf{P}_{\text{NOC}}^T \quad (3)$$

210 From the PCA model built with NOC batches, two MSPC control charts can be built,
 211 in which observations of new batches are represented: a) Hotelling's T^2 chart, usually referred
 212 as D -statistic ($D_{\text{stat.}}$), represents the estimated Mahalanobis distance from the center of the
 213 latent subspace, representing the average in control conditions of a batch, to the projection of
 214 a new batch (or observation) onto this subspace and the b) Q -statistic chart ($Q_{\text{stat.}}$)accounts
 215 for the residual part of the process variation not explained by the PCA model.

216 The Hotelling statistic, $D_{\text{stat.}}$, was calculated using the following equation:

$$D_{stat.} = \mathbf{t}^T \boldsymbol{\Theta}^{-1} \mathbf{t} \quad (4)$$

217 Where \mathbf{t} is the vector containing the scores of a new given batch with the A retained
 218 principal components (PC's), and $\boldsymbol{\Theta}$ is the scores covariance matrix with $(A \times A)$ size. The
 219 control limit for this chart is calculated according to the equation proposed by Jackson [35].

$$D_{CL} = \frac{A(I-1)}{I-A} F(A, I-A, \alpha) \quad (5)$$

220 where I is the number of in control batches used to build the model with A PC's and $F(A, I -$
 221 $A, \alpha)$ is the $100(1 - \alpha)$ percentile of the corresponding F distribution.

222 The $Q_{stat.}$ for the i th new batch \mathbf{x}_i is given by

$$Q_{stat.} = \mathbf{e}_i^T \mathbf{e}_i \quad (6)$$

223 where \mathbf{e}_i is the residual vector of the i th new batch from the PCA model. Regarding the
 224 control limit for the $Q_{stat.}$ chart, Jackson and Mudholkar[36] showed that an approximate
 225 $Q_{stat.}$ critical value at significance level α is given by

$$Q_{CL} = \theta_1 \left[\frac{z_\alpha \sqrt{2\theta_2 h_0^2}}{\theta_1} + 1 + \frac{\theta_2 h_0 (h_0 - 1)}{\theta_1^2} \right]^{1/h_0} \quad (7)$$

226 where, $\theta_k = \sum_{j=A+1}^{rank(X)} \lambda_j^k$ and $h_0 = 1 - (2\theta_1 \theta_3 / 3\theta_2^2)$, λ_j are the eigenvalues of the PCA
 227 residual covariance matrix and z_α is the $100(1 - \alpha)\%$ standardized normal percentile.

228 Two MSPC approaches were applied in this work, devoted to off-line and on-line
 229 control, respectively. Both approaches and related control charts are explained below.

230 Off-line batch MSPC

231 Off-line batch MSPC charts were built using data provided from completed distillation
 232 processes. Different models were built according to the starting information used, either
 233 temperatures from distillation curves or information derived from NIR spectra, Figure 4.

234 **(Insert Figure 4)**

235 **a) Off-line batch MSPC models using distillation curves**

236 The distillation curves from the 9 NOC distillation batches were arranged in a matrix
 237 $(I \times K)$, with $I = 9$ rows and $K = 86$ observation points of the distillation curve. This matrix
 238 was mean-centered and decomposed by PCA to obtain the model loadings and MSPC limits,

239 see Figure 4(a). New batch data were projected into the model to obtain the related statistical
240 parameters ($D_{stat.}$ and $Q_{stat.}$).

241 **b) Off-line batch MSPC models using NIRS data**

242 Different off-line MSPC models were built with the NIRS-derived information. All
243 models were built on data sets with $I = 9$ rows and a variable number of columns depending
244 on the kind of NIRS-derived information, see Figure 4(b). This gave rise to three different
245 MSPC models:

246 i. **Models based on the original preprocessed NIR data matrix.** This
247 model is done using a matrix containing the NIR readings from each
248 individual NOC batch row-wise unfolded into a vector, i.e. the matrix of a
249 batch with dimensions ($K \times J$), where $K = 86$ are batch observation points
250 and $J = 573$ wavelengths, is arranged in a row vector with dimension (1
251 $\times KJ$), with $K = 86$ and $J = 573$. Then, the information of $I = 9$ NOC
252 batches was arranged in a matrix sized ($I \times KJ$), on which the MSPC model
253 was built.

254 ii. **Models based on the batch scores from PCA decomposition of the**
255 **NOC multiset structure.** The information of a NOC batch are the scores
256 obtained in the PCA model of the related NIR spectra, row-wise unfolded
257 into a vector sized ($1 \times KA$) with A being the number of retained principal
258 components. Then, the information of $I = 9$ NOC batches was arranged in a
259 matrix sized ($I \times KA$), on which the MSPC model was built.

260 iii. **Models based on the resolved concentration profiles from MCR-ALS**
261 **decomposition of the NOC multiset structure.** The information of a
262 NOC batch are the concentration profiles obtained in the MCR-ALS model
263 of the related NIR spectra, row-wise unfolded into a vector sized ($1 \times KN$)
264 with N being now the number of MCR contributions needed to describe the
265 process. Then, the information of $I = 9$ NOC batches was arranged in a
266 matrix sized ($I \times KN$), on which the MSPC model was built. Please note
267 that, generally speaking, the use of only some of the concentration profiles
268 modeled in a batch could be an option to build the MSPC model, provided
269 that the selected profiles were proven to be very specific indicators of the

270 process evolution or that the discarded profiles belonged to spurious
271 process contributions, e.g., modeled background contributions if existing.
272 Please note that even if the use of C-profiles implies a noise-filtered
273 compression of the original information, the size of the unfolded profiles,
274 sized ($1 \times KN$) per each NOC batch, requires a PCA-based MSPC model
275 for easier interpretability.

276 The MSPC PCA models built with the different kinds of starting information were
277 used to extract the related $D_{stat.}$ and $Q_{stat.}$ charts limits. Suitable data from new batches, not
278 used to build the model, were projected onto the MSPC PCA model to test the performance of
279 the models built.

280 On-line batch MSPC

281 Different on-line MSPC monitoring charts were developed using the data provided
282 from NIRS measurements. As in the off-line approach, the same unfolded NOC matrix with
283 the original NIR variables was used in the on-line approach. However, three on-line MSPC
284 approaches were proposed using multiple PCA models based on different intervals of
285 observation points, as described below:

286 a) On-line MSPC based on individual process observation models

287 This approach is the most straightforward method. An individual model is built per
288 each observation point using historical data from on-specification completed batches as
289 illustrated in Figure 5(a). Thus, during a new batch, the new on-line data obtained (NIR
290 spectrum of current observation) is projected into the respective observation point model and
291 the statistical parameters compared with the control chart limits.

292 **(Insert Figure 5)**

293 b) On-line MSPC based on Evolving MSPC models

294 MSPC models with increasing number of observation points are built adding the new
295 current distillation point in every new model until all distillation process is covered. As
296 illustrated in Figure 5(b), the first MSPC model is built using only the NIRS data matrix of
297 the NOC historical data batches at the first recovered point (5 wt%), the second model using
298 two observation points (5 and 6 wt%) and so on. For new batch monitoring, the data up to the
299 current observation point are projected into the model for the related observations points and
300 statistically tested.

301 c) On-line MSPC based on Fixed Size Moving Window, FSMW-MSPC, models

302 Several MSPC models built with a fixed size window (FSMW) including the current
303 observation and several consecutive past observation points are built using the NOC historical
304 data. The window slides one observation ahead in each new model until all observation points
305 are covered. For instance, in Figure 5(c) the window moves from k to $k = k + 1$ and so on
306 until $k = K$. For new batch monitoring, the data from the observation points covered by the
307 moving window are projected into the model for the respective observations points and
308 statistically tested.

309 The three approaches aim at on-line process control, but there are important differences
310 due to the use of the different information in the models. Thus, the modality looking at
311 individual process points does not take into account the neighbouring past observations and,
312 hence, the evolution of the process. In the modalities FSMW-MSPC and evolving MSPC, the
313 process evolution is taken into account and not only the new process observation of interest.
314 In the case of the FSMW-MSPC model, only the recent past observation points (those within
315 the window) are taken into account and the window size established is related to the number
316 of relevant neighbouring process observations. Instead, the evolving-MSPC takes into
317 account all process evolution until the present observation, giving potentially the same
318 importance to all the past observations analyzed.

319 **4. Results and discussion**

320 ***4.1. Visual interpretation of distillation curve and NIR process data***

321 Prior to chemometric analysis, the distillation curve and raw NIR spectra obtained
322 during the distillation process were visually interpreted. Figure 2(a) illustrates the distillation
323 curve of an on-specification batch (B07), the related process raw NIR spectra, Figure 2(b),
324 and NIR spectra selected at four specific distillation points, Figure 2(c).

325 A sudden change in temperature can be observed through a simple visual inspection of
326 the distillation curve between 60 and 70 wt%. This behavior is observed in gasoline-ethanol
327 blends due to the formation of azeotropes of ethanol and hydrocarbons [37–40]. Distillation
328 curve for gasoline-ethanol blend show three distinct regions: a plateau or azeotropic region
329 (ethanol–hydrocarbon azeotropes are boiled) in the beginning of the distillation process, a
330 transition region (sudden change in temperature) and a dilution-only region at the end of the
331 distillation (after all added ethanol is boiled-off), as observed by French and Malone[38].

332 Four observation points (10, 50, 70 and 90 wt%) at the start and end of each
333 distillation region were chosen to visualize the changes in NIR spectra with the evolution of
334 distillation process. Figure 2(c) shows the complexity of the many superimposed absorption
335 bands of the NIR spectra acquired during the distillation process. The bands around 1180 nm
336 correspond to the second overtone, around 1400 nm to the 1st overtone combination and
337 around 1700 nm to the first overtone region of carbon-hydrogen (C-H) bonds present in all
338 points observed. The band around 2080 nm observed in the fractions at 10 and 50 wt% is
339 related to the absorption of a combination of oxygen-hydrogen (O-H) stretching and bending
340 from ethanol added to the gasoline. An absorbance increment in the band around 2080 nm
341 was observed as the distillation was evolving from 10 to 50 wt%, mainly related to the
342 increase of the ethanol relative concentration in the distilled fractions. A new band around
343 2170 nm appears in the spectra of the fraction at 70 and 90 wt%. This new band is related to
344 absorption of aromatic compounds in the heavy fractions of the gasoline [41–43].

345 ***4.2. Process modeling of NIR data***

346 **Global process description (PCA model)**

347 The NIR data were mean-centered and decomposed by PCA. Venetian blinds cross-
348 validation method was used to find the number of principal components. 3 principal
349 components explained 98.98 % (PC1 84.64%, PC2 13.11% and PC3 1.23%) representing a
350 good summary of batch variability.

351 Figure 6(a) shows the principal components score plot distribution for PC1 and PC2
352 extracted from NIRS data of batches B01-09 used to build the PCA model (blue dots). The
353 distribution of scores illustrates the process trajectory of on-specification batches and its
354 variability. Because of the unstable distillation rate at the start of the distillation process, more
355 variation was observed in these observation points as compared to the rest of the process. In
356 addition, the NIRS data collected from the distillations of on-specification gasoline batch
357 B11, not used in the PCA process modeling, and off-specification batch B13, which had only
358 15 % (v/v) of ethanol added, were projected in the PCA model. The scores obtained from PCA
359 projection allowed the observation of the process trajectory of the new projected batches.
360 Batch B11 (in magenta circles) was observed to follow the same on-specification process
361 trajectory, while batch B13 (in red triangles) deviated from NOC trajectory, as illustrated in
362 Figure 6(a). On-specification batch B10 when projected to the PCA model showed the same
363 behavior as B11. Off-specification batches B12, B14-23 also deviate from NOC trajectory as

364 batch B13, (data not shown for clarity). The deviation becomes larger when the ethanol
365 content is further from the ethanol specification level of NOC batches.

366 MCR-ALS

367 The dataset decomposition through MCR-ALS provides a model of process
368 components easy to interpret and complementary to the global process description provided
369 by PCA. The multibatch structure with the preprocessed (not mean-centered) data obtained
370 from the distillation batches was decomposed by MCR-ALS. Four components were found
371 through singular value decomposition, which agrees with the three contributions found in
372 PCA of mean-centered data, since the rank decreases in one when mean centering is
373 performed.

374 The four components concentration (distillation) and spectral profiles obtained after
375 MCR-ALS decomposition of the multiset structure are shown in Figure 6(b). The components
376 resolved from the distillation process are related to the main distilled fractions of gasolines
377 “type C”: First, light hydrocarbons; second, ethanol; third and fourth, mid to high molecular
378 weight (MW) hydrocarbons and aromatic compounds, as reported elsewhere [44]. The
379 identity of these compounds is confirmed when looking at the spectral features found in the
380 related pure spectra and at the temperature distillation range.

381 The low MW hydrocarbons fraction is mainly distilled together with ethanol as
382 azeotropes at the beginning of the distillation, i.e., at lower temperatures, as observed in the
383 concentration profiles of components (1) and (2), see Figure 6(b). After 70 wt% of the
384 distillation process, almost all ethanol, component (2), was boiled-off remaining most of the
385 mid to high MW fractions of gasoline, rich in aromatic compounds, components (3) and (4).
386 This region was observed in the distillation curves and is characterized by an increase in the
387 slope of the distillation curve, as observed in Figure 2(a).

388 For comparison, Figure 6(b) shows the distillation profiles of B13 (with only 15
389 %(v/v) ethanol). Although the component spectra are the same, all distillation profiles are
390 shifted to lower wt% of distillate, as expected for a batch with lower ethanol content.

391 **4.3. Process control**

392 **Off-line batch process control**

393 Off-line batch MSPC charts were built working with data coming from completed
394 distillation batches. Specificity and sensitivity were adopted as quality parameters to assess
395 the performance of MSPC charts for off-line batch process control. Specificity stands for the
396 ratio of NOC batches (on-specification) correctly identified over the total NOC batches used
397 to test the MSPC charts. Sensitivity is derived as the ratio of out of NOC (off-specification)
398 batches correctly identified as out of NOC over the total out of NOC tested.

399 **Process control starting information**

400 The starting information used to build off-line batch MSPC models came either from
401 distillation curves or NIR process data. The different starting information is depicted in
402 section 3.2. Full distillation curves or observations within a selected temperature range were
403 used to build off-line PCA-based MSPC models. Derivative form of the distillation curves
404 was also used to improve the models. As for NIR information, full original preprocessed NIR
405 spectra or selected spectral ranges were used to build the models. MSPC models were also
406 built with the PCA scores, extracted from the process modeling by PCA, with all the
407 distillation concentration profiles or only with the component related to ethanol, extracted
408 from MCR-ALS decomposition, as described in section 3.2.

409 **Off-line batch MSPC results**

410 Table 2 shows the summary of the results using the different starting information to
411 build and test off-line batch MSPC models.

412 **(Insert Table 2)**

413 An MSPC PCA model with mean-centered full distillation curve data (5-90 wt%)
414 from NOC batches was built with 2 PC's and explained 90.91 % of data variance. MSPC
415 chart based on $Q_{stat.}$ parameter correctly identified NOC and off-spec batches used to test the
416 control charts as observed in Table 2 (row #1 has 100% specificity and sensitivity of $Q_{stat.}$).
417 However, despite $D_{stat.}$ chart correctly identifies NOC batches, some off-spec batches are
418 below the $D_{stat.}$ limit, see Figure 7(b), the sensitivity observed was **73.33%**, Table 2 row #1.
419 This may have happened because distillation curves of off-specification batches with ethanol
420 concentration near to the on-specification level, 27 %(v/v), have extensive distillation ranges

421 with similar behavior (except for the points in the steepest zone of the curve) and, when
422 considered the full curve, stay within the accepted variability of the NOC batches.

423 Another PCA model was built using the same data used previously, but this time
424 preprocessed by Savitzky-Golay derivative and mean-centered. Results showed an
425 improvement on the sensitivity, but still some batches were misidentified in the $D_{stat.}$ chart, as
426 reported in Table 2 row #2. All off-specification batches could be correctly identified using
427 the derivative curve data only in the distillation range between 25 and 75 wt%, (Table 2 row
428 #3). This range showed most of the variation in the distillation curves due to different ethanol
429 content and avoided the unstability and, hence, undesired and non-composition related
430 variability in the beginning of the distillation.

431 As observed in the MSPC charts built with the distillation curve data, the specificity
432 and sensitivity of the $Q_{stat.}$ charts for all models built with NIRS data were 100%. However,
433 different strategies were necessary to improve the sensitivity of $D_{stat.}$ MSPC charts.

434 The off-line PCA-based batch MSPC charts built using information from NIR spectra
435 are explained below. Table 2, row #4, shows the results from a model built using the full
436 preprocessed spectra (1103 – 2228 nm) and distillation (5-90 wt%) range. Despite of the
437 100% specificity in $Q_{stat.}$ chart, none of the off-specification batches was detected as faulty
438 by the $D_{stat.}$ chart. The $D_{stat.}$ MSPC chart sensitivity was significantly improved to 75%
439 when the NIRS data were reduced taking only the NIR observations within the distillation
440 range from 60 wt% to 70 wt%, see Table 2, row #5. NIRS data were also reduced by selecting
441 the most expressive spectral bands related mainly to hydrocarbons (1600-1800 nm) and
442 ethanol absorption regions (2000-2200 nm). The MSPC chart built with this reduced spectral
443 and distillation range improved the $D_{stat.}$ sensitivity to 83% (row #6), but still some samples
444 with composition similar to the on-specification batches were missed by the control chart.

445 Off-line MSPC models were built with the NIR information compressed by PCA and
446 MCR-ALS. Similar results were observed. The sensitivity for $D_{stat.}$ MSPC charts built with
447 concatenated PCA scores or MCR-ALS concentration profiles (row #7 and #10) improved
448 when compared with full spectral and distillation range data without data compression (row
449 #4), see Table 2. MSPC models built with the compressed information extracted from the
450 NIR observations within the 60-70 wt% distillation range showed an expressive improvement
451 of the $D_{stat.}$ sensitivity to 91.67% (row #8 and #11). $D_{stat.}$ charts (row #9 and #12) showed
452 100% sensitivity when MSPC models were built using the Savitzky-Golay derivative of the

453 PCA scores or the MCR-ALS concentration profiles within the same distillation range (60-
454 70%). MSPC models were built also using only the ethanol distillation profile. Results are
455 show in Table 2, rows #13 and #14. The $D_{stat.}$ sensitivity was higher than in models built
456 with all four components for models built with the full distillation range. Moreover, when the
457 derivative ethanol profile in the 60-70 wt% distillation range, 100 % specificity in $D_{stat.}$ chart
458 was achieved. The improvement of results when using only the ethanol concentration profile
459 might be related to the better definition of this compound in the MCR-ALS results.

460 **On-line batch MSPC on the NIR data**

461 On-line batch MSPC control charts were built following the strategies described in
462 section 3.2. For the distillation batches studied, PCA models were calculated for each
463 observation point (86 models) following each one of the strategies described using the mean-
464 centered data collected from NOC batches. Individual observation models (see Figure 5(a))
465 and evolving models (see Figure 5(b)) were calculated as described. For FSMW evolving
466 models (see Figure 5(c)), the window selected enclosed 15 neighbouring observations. Thus,
467 for observations nr. 1 to 14, PCA models were calculated as in the evolving strategy (see
468 Figure 5(b)), whereas from observation nr. 15 and on, the full sliding window of 15 points
469 was applied, as seen in Figure 5(c). PCA models for individual observation and FSMW
470 evolving strategies were built with one principal component for all observation points, while
471 in evolving models, one PC was used in evolving models from 5 to 20 wt% and three PC's in
472 the remaining observation points. A confidence interval of 99% was considered to calculate
473 the MSPC charts limits, $D_{CL99\%}$ and $Q_{CL99\%}$, for each model, as described earlier in section
474 3.2.

475 The NIR measurements for a new batch observation were mean-centered according to
476 the mean of NOC batches and each observation (or set of observations) projected into the
477 PCA model built for each strategy to extract the MSPC statistics, $D_{stat.}$ and $Q_{stat.}$.

478 At this point, it is important to stress the difference between off-line and on-line
479 MSPC control charts.

480 Off-line MSPC control charts are based on a single PCA model built on the completed
481 NOC batches. The final $D_{stat.}$ and $Q_{stat.}$ charts represent the values of these statistics vs. the
482 batch index of each analyzed new batch. Every new batch is represented by a point.

483 On-line MSPC control charts display simultaneously the information of many PCA
484 models, as many as observations in each batch, see Figure 5. Therefore, each new observation
485 (NIR spectrum) acquired in a new batch is tested to see whether it is in- or out of control on a
486 different PCA model. The process control is done at an observation level and not at a full
487 batch level, as in the off-line approach. As a consequence, every new batch has a full $D_{stat.}$
488 and a full $Q_{stat.}$ plot, where the x-axis refers now to the different observations studied along
489 the process evolution.

490 Control limits in $D_{stat.}$ and $Q_{stat.}$ would change per each new observation analyzed,
491 since a different PCA model is used for projection every time. To facilitate visualization, the
492 y-axis represents scaled values of $D_{stat.}$ and $Q_{stat.}$, defined as $D_{stat.}/D_{CL}$ and $Q_{stat.}/Q_{CL}$. In
493 this way, a flat line at value 1 represents the control limits for all models used in $D_{stat.}$ and
494 $Q_{stat.}$ for all observations. On-line $D_{stat.}$ and $Q_{stat.}$ charts, which represent the evolution of
495 the related scaled statistics as a function of the observation (% distillate) analyzed, allow not
496 only identifying on- and off-specification batches, but to know when the anomaly in an
497 abnormal batch starts.

498 The results after monitoring new batches through the three different on-line MSPC strategies
499 (individual observation model, FSMW MSPC evolving models and evolving MSPC models)
500 are summarized in Table 3. Table 3 shows whether a new batch was diagnosed as on-
501 specification or not and which MSPC chart ($D_{stat.}$, $Q_{stat.}$ or both) detected the fault. (Please
502 note that the behavior of the full distillation batch is analyzed in this section for a better
503 comparison of the three approaches. In a real on-line control context, the distillation would be
504 stopped as soon as found to be out of specification).

505 Observing the information summarized in Table 3, $Q_{stat.}$ on-line MSPC charts
506 detected correctly a fault in all off-specification batches by using any of the three on-line
507 strategies. $D_{stat.}$ charts worked generally well, except when using evolving models, which
508 were not able to detect fault in off-specification batches with ethanol content very
509 approximate to the accepted specification and above, i.e. batches B17 to B23, see Table 1 and
510 3. The on-specification batch B11 was wrongly detected as faulty by the $Q_{stat.}$ on-line MSPC
511 chart using the individual observation model MSPC strategy.

512 **(Insert Table 3)**

513 Figure 8 shows the D and Q statistics on-line control charts from distillation batches
514 B11 (on-specification, with 27% ethanol added) and B18 (off-specification, with 25% ethanol
515 added) for the three different on-line batch MSPC strategies.

516 Some comments need to be done for each on-line strategy according to the observed
517 results.

518 a) Individual process observation models

519 Q_{stat} . MSPC charts were observed to be very sensitive to fault detection. Besides, they
520 show clearly the point where the batch starts to be anomalous. However, Q_{stat} . charts were
521 more prone to show false alarms, Figure 8(a). This happens because each model was built
522 using a single observation point and a slight variation in an individual observation for a new
523 batch process leads to a fault detection.

524 b) Evolving MSPC models

525 The evolving MSPC strategy considered the evolution of the process since the start,
526 building models with increasing number of observations. This caused less sensitive D_{stat} .
527 charts, since past NOC observations may have a lot of weight in the models and batches can
528 be detected easily as faulty only when the fault observations occurred at the beginning of the
529 distillation process (batches B11-16). Batches with ethanol concentration near to the
530 specification value and above were not detected by D_{stat} . charts since the fault occurred too
531 late and was not large enough to compensate the weight of the large number of initial NOC
532 observations. Despite of this fact, the evolution of D_{stat} . values for undetected off-
533 specification batches show a different trend (a clear increase when the abnormal behavior
534 starts) as compared to on-specification batches (presenting a flat constant tendency), as
535 observed in D_{stat} . charts Figure 8(b). This may suggest that the D_{stat} . chart could still be used
536 in these instances if the control limits were set empirically. Q_{stat} . charts performed more
537 satisfactorily in fault detection. However, faults were detected later than in individual
538 observation models due to the excessive weight of past NOC observations as well.

539 c) Fixed size moving window, FSMW-MSPC models

540 The FSMW strategy considered only a few past observation points, set according to
541 the window size (15 observations were used in this study). This feature produced more
542 sensitive D_{stat} . charts because past NOC observations had less weight in models, Figure 8(c).
543 FSMW strategy was observed to be less prone to false alarms on Q_{stat} . charts than individual

544 observation charts, Figure 8(a), since individual point fluctuations have less impact in the
545 window-based PCA models. This strategy has been found to be the most flexible of the three,
546 showing efficient and easy detection of faults and avoiding false alarms. Obviously the
547 performance of this approach may depend on the width of the window: if too small, false
548 alarms may show up in analogy to what happens in individual observation models; if too big,
549 sensitivity in $D_{stat.}$ chart may decrease because of the weight of too many past NOC
550 observations in the chart. This inconvenient is clearly surmountable if the window width is set
551 by using representative off-spec batches that may allow setting the correct window width to
552 avoid the malfunctions described in the other two on-line MSPC approaches.

553 **5. Conclusions**

554 The present work provides an improvement of PAT technologies for distillation-based
555 quality control procedures through the design of an automatic distillation device that allowed
556 synchronized measurements of the distilled mass percentage, distillation temperature and
557 NIR spectra during the distillation process.

558 Process modeling on NIR spectra by PCA and MCR-ALS allowed understanding the
559 process evolution from a global (scores plot) and component-wise (distillation profiles) point
560 of view, respectively. In this sense, MCR-ALS provides a good thermal and physicochemical
561 characterization of distilled fractions, even if coming from a simple distillation process.

562 MSPC strategies based on the different kinds of data obtained from the designed
563 device are proposed. Off-line models using distillation curves were able to detect off-
564 specification batches when suitable preprocessing and distillation curve range were used.
565 Successful off-line MSPC models were built with the NIR spectra information compressed
566 into PCA scores or MCR-ALS concentration profiles. The possibility to perform a sensible
567 selection of some of the MCR-ALS concentration profiles, linked to particularly relevant
568 process contributions has proven to improve MSPC results.

569 On-line batch MSPC strategies were proposed for fault detection during the
570 distillation process using the collected NIRS data. Individual process observations MSPC
571 models showed $D_{stat.}$ charts very sensitive to fault detection; however, false alarms were
572 observed in the $Q_{stat.}$ charts. Evolving MSPC models were able to solve the false alarms
573 observed with the individual observation strategy, but failed to detect some off-specification
574 batches with similar composition to NOC batches when using $D_{stat.}$ charts. The FSMW-
575 MSPC approached used a flexible combination of the other two strategies and succeeded to

576 detect all off-specification batches and correctly identify on-specification batches during the
577 test with both $D_{stat.}$ and $Q_{stat.}$ control charts, avoiding false alarms.

578 **6. Acknowledgements**

579 R.R. de Oliveira acknowledges the EMQAL Grant. EMQAL is a Joint European
580 Master Programme selected under Erasmus Mundus coordinated by University of Barcelona.
581 Funding support from the European Community's Framework programme for Research and
582 Innovation Horizon 2020 SPIRE - Integrated Process Control (ProPAT), grant Agreement no.
583 637232 and Spanish government through project CTQ2015-66254-C2-2-P are also
584 acknowledged. K.M.G. Lima acknowledges the CNPq (Grant 305962/2014-4) for financial
585 support. A.O. Sousa acknowledges the PETROBRAS (Grant 2012/00217-7) for financial
586 support.

- 588 [1] ASTM D86-15, Standard Test Method for Distillation of Petroleum Products and
589 Liquid Fuels at Atmospheric Pressure, in: ASTM B. Stand., 2015.
- 590 [2] C. Pasquini, S.H.F. Scafi, Real-Time Monitoring of Distillations by Near-Infrared
591 Spectroscopy, *Anal. Chem.* 75 (2003) 2270–2275.
- 592 [3] V.A. Corro-Herrera, J. Gómez-Rodríguez, P.M. Hayward-Jones, D.M. Barradas-
593 Dermitz, M.G. Aguilar-Uscanga, A.C. Gschaedler-Mathis, *In-situ* monitoring of
594 *Saccharomyces cerevisiae* ITV01 bioethanol process using near-infrared spectroscopy
595 NIRS and chemometrics, *Biotechnol. Prog.* 32 (2016) 510–517.
- 596 [4] H. Xiong, X. Gong, H. Qu, Monitoring batch-to-batch reproducibility of liquid-liquid
597 extraction process using in-line near-infrared spectroscopy combined with multivariate
598 analysis, *J. Pharm. Biomed. Anal.* 70 (2012) 178–187.
- 599 [5] RESOLUÇÃO ANP N^o 40, DE 25.10.2013 DOU 28.10.2013,
600 [http://nxt.anp.gov.br/NXT/gateway.dll/leg/resolucoes_anp/2013/outubro/ranp_40_2013.xml?f=templates\\$fn=document-frame.htm\\$3.0\\$q=\\$x=\\$nc=2230](http://nxt.anp.gov.br/NXT/gateway.dll/leg/resolucoes_anp/2013/outubro/ranp_40_2013.xml?f=templates$fn=document-frame.htm$3.0$q=$x=$nc=2230). Accessed
601 August 1, 2016.
- 602
- 603 [6] S. Wold, K. Esbensen, P. Geladi, Principal component analysis, *Chemom. Intell. Lab.*
604 *Syst.* 2 (1987) 37–52.
- 605 [7] R. Tauler, M. Maeder, A. de Juan, Multiset Data Analysis: Extended Multivariate
606 Curve Resolution, in: *Compr. Chemom. Chem. Biochem. Data Anal. Four-Volume Set.*
607 Vol. 2, Chapter 2.24, S.D. Brown, R. Tauler, B. Walcz., Elsevier, 2009: pp. 473–505.
- 608 [8] Y. Jin, Z. Wu, X. Liu, Y. Wu, Near infrared spectroscopy in combination with
609 chemometrics as a process analytical technology (PAT) tool for on-line quantitative
610 monitoring of alcohol precipitation, *J. Pharm. Biomed. Anal.* 77 (2013) 32–39.
- 611 [9] M.C. Sarraguça, P.R.S. Ribeiro, A.O. dos Santos, J.A. Lopes, Batch Statistical Process
612 Monitoring Approach to a CocrySTALLIZATION Process, *J. Pharm. Sci.* 104 (2015) 4099–
613 4108.
- 614 [10] H. Howland, S.W. Hoag, Analysis of curing of a sustained release coating formulation
615 by application of NIR spectroscopy to monitor changes physical-mechanical
616 properties, *Int. J. Pharm.* 452 (2013) 82–91.
- 617 [11] R. Kona, H. Qu, R. Mattes, B. Jancsik, R.M. Fahmy, S.W. Hoag, Application of in-line
618 near infrared spectroscopy and multivariate batch modeling for process monitoring in
619 fluid bed granulation, *Int. J. Pharm.* 452 (2013) 63–72.
- 620 [12] T. Kourti, J.F.J.F. MacGregor, Process analysis, monitoring and diagnosis, using
621 multivariate projection methods, *Chemom. Intell. Lab. Syst.* 28 (1995) 3–21.
- 622 [13] A. AlGhazzawi, B. Lennox, Monitoring a complex refining process using multivariate
623 statistics, *Control Eng. Pract.* 16 (2008) 294–307.
- 624 [14] A. AlGhazzawi, B. Lennox, Model predictive control monitoring using multivariate
625 statistics, *J. Process Control* 19 (2009) 314–327.
- 626 [15] T.C. Ávila, R.J. Poppi, I. Lunardi, P.A.G. Tizei, G.A.G. Pereira, Raman spectroscopy
627 and chemometrics for on-line control of glucose fermentation by *Saccharomyces*
628 *cerevisiae*, *Biotechnol. Prog.* 28 (2012) 1598–1604.

- 629 [16] J. Alves-Rausch, R. Bienert, C. Grimm, D. Bergmaier, Real time in-line monitoring of
630 large scale Bacillus fermentations with near-infrared spectroscopy, *J. Biotechnol.* 189
631 (2014) 120–128.
- 632 [17] H. Huang, H. Qu, In-line monitoring of alcohol precipitation by near-infrared
633 spectroscopy in conjunction with multivariate batch modeling, *Anal. Chim. Acta* 707
634 (2011) 47–56.
- 635 [18] P. Nomikos, J.F. MacGregor, Multivariate Statistical Process Control Charts for
636 Monitoring Batch Processes, *Technometrics* 37 (1995) 41–59.
- 637 [19] P. Nomikos, J.F. MacGregor, Monitoring batch processes using multiway principal
638 component analysis, *AIChE J.* 40 (1994) 1361–1375.
- 639 [20] P. Nomikos, J.F. MacGregor, Multi-way partial least squares in monitoring batch
640 processes, *Chemom. Intell. Lab. Syst.* 30 (1995) 97–108.
- 641 [21] S. Wold, N. Kettaneh, H. Friden, A. Holmberg, Modelling and Diagnostics of Batch
642 Processes and Analogous Kinetic Experiments, *Chemom. Intell. Lab. Syst.* 44 (1998)
643 331–340.
- 644 [22] S. Rännar, J.F. MacGregor, S. Wold, Adaptive batch monitoring using hierarchical
645 PCA, *Chemom. Intell. Lab. Syst.* 41 (1998) 73–81.
- 646 [23] L. Zhao, T.-Y. Chai, G. Wang, A Nonlinear Modeling and Online Monitoring Method
647 for the Batch Process Using Multiple Local PCA, (2003) 2–5.
- 648 [24] L. Zhao, T. Chai, Adaptive moving window MPCA for online batch monitoring, in:
649 2004 5th Asian Control Conf., 2004: p. 1290–1295 Vol.2.
- 650 [25] M. Maeder, Evolving Factor Analysis for the Resolution of Overlapping
651 Chromatographic Peaks, *Anal. Chem.* 59 (1987) 527–530.
- 652 [26] M. Maeder, A. de Juan, Two-Way Data Analysis: Evolving Factor Analysis, *Compr.*
653 *Chemom.* 2 (2010) 261–274.
- 654 [27] A. Savitzky, M.J.E. Golay, Smoothing and Differentiation of Data by Simplified Least
655 Squares Procedures., *Anal. Chem.* 36 (1964) 1627–1639.
- 656 [28] A. de Juan, J. Jaumot, R. Tauler, Multivariate Curve Resolution (MCR). Solving the
657 mixture analysis problem, *Anal. Methods* 6 (2014) 4964.
- 658 [29] A. de Juan, R. Tauler, Chemometrics applied to unravel multicomponent processes and
659 mixtures, *Anal. Chim. Acta* 500 (2003) 195–210.
- 660 [30] R. Tauler, B.R. Kowalski, S. Fleming, Multivariate Curve Resolution Applied to
661 Spectral Data from Multiple Runs of an Industrial Process, *Anal. Chem.* 65 (1993)
662 2040–2047.
- 663 [31] W. Windig, J. Guilment, Interactive Self-Modeling Mixture Analysis, *Anal. Chem.* 63
664 (1991) 1425–1432.
- 665 [32] J. Jaumot, A. de Juan, R. Tauler, MCR-ALS GUI 2.0: New features and applications,
666 *Chemom. Intell. Lab. Syst.* 140 (2014) 1–12.
- 667 [33] T. Kourti, 4.02 - Multivariate Statistical Process Control and Process Control, Using
668 Latent Variables, in: *Compr. Chemom.*, 2009: pp. 21–54.
- 669 [34] S. Wold, Cross -Validatory Estimation of the Number of Components in Factor and
670 Principal Components Models, *Technometrics* 20 (1978) 397–405.

- 671 [35] J.E. Jackson, *A User's Guide to Principal Components*, Wiley, New York, 1991.
- 672 [36] J.E. Jackson, G.S. Mudholkar, Control Procedures for Residuals Associated with
673 Principal Component Analysis, *Technometrics* 21 (1979) 341–349.
- 674 [37] E. V. Takeshita, R.V.P. Rezende, S.M.A.G.U. de Souza, A.A.U. de Souza, Influence of
675 solvent addition on the physicochemical properties of Brazilian gasoline, *Fuel* 87
676 (2008) 2168–2177.
- 677 [38] R. French, P. Malone, Phase equilibria of ethanol fuel blends, 229 (2005) 27–40.
- 678 [39] R.M. Balabin, R.Z. Syunyaev, S.A. Karpov, Quantitative measurement of ethanol
679 distribution over fractions of ethanol-gasoline fuel, *Energy and Fuels* 21 (2007) 2460–
680 2465.
- 681 [40] V.F. Andersen, J.E. Anderson, T.J. Wallington, S.A. Mueller, O.J. Nielsen, Distillation
682 curves for alcohol-gasoline blends, *Energy and Fuels* 24 (2010) 2683–2691.
- 683 [41] Z. Xiaobo, Z. Jiewen, M.J.W. Povey, M. Holmes, M. Hanpin, Variables selection
684 methods in near-infrared spectroscopy, *Anal. Chim. Acta* 667 (2010) 14–32.
- 685 [42] C. Pasquini, *Near Infrared Spectroscopy: fundamentals, practical aspects and analytical*
686 *applications*, *J. Braz. Chem. Soc.* 14 (2003) 198–219.
- 687 [43] D.A. Burns, E.W. Ciurczak, *Handbook of near-infrared analysis*, 3rd ed., *Anal.*
688 *Bioanal. Chem.* 393 (2009) 1387–1389.
- 689 [44] J.L. Burger, N. Schneider, T.J. Bruno, Application of the advanced distillation curve
690 method to fuels for advanced combustion engine gasolines, *Energy and Fuels* 29
691 (2015) 4227–4235.
- 692

8. List of Tables

Table 1 Description of Batch ID and their related composition, as used in this work.

Table 2 Off-line batch MSPC results.

Table 3 On-line batch MSPC results on test batches B10-23.

Table 1 Description of Batch ID and their related composition, as used in this work.

Batch ID	%(v/v) Gasoline	%(v/v) Ethanol	Class
B01-B11	73	27	On-specification
B12	90	10	
B13	85	15	
B14-B16	80	20	
B17-B18	75	25	Off-specification
B19-B20	70	30	
B21-B22	65	35	
B23	60	40	

Table 2 Off-line batch MSPC results.

#	Description	NC	%EV	%Specificity		%Sensitivity	
				$D_{stat.}$	$Q_{stat.}$	$D_{stat.}$	$Q_{stat.}$
Distillation Curves							
1	DistRange (5-90 wt%)	2	90.91	100	100	66.67	100
2	DistRange(5-90 wt%)_1 st diff.SG	2	94.83	100	100	91.67	100
3	DistRange(25-75 wt%)_1 st diff.SG	2	98.36	100	100	100	100
NIR information							
Unfolded NIRS data							
4	FullSpec_DistRange(5-90%)	3	68.91	100	100	0.00	100
5	FullSpec_DistRange(60-70%)	2	92.56	100	100	75.00	100
6	SelSpec_DistRange(60-70%)	2	94.54	100	100	83.33	100
scores from PCA modelling (3 PC's)							
7	DistRange(5-90%)	2	87.53	100	100	66.67	100
8	DistRange(60-70%)	2	96.52	100	100	91.67	100
9	DistRange(60-70%)_1 st diff.SG	2	98.67	100	100	100	100
C profiles from MCR-ALS modelling (4comp)							
10	DistRange(5-90%)	2	81.07	100	100	33.3	100
11	DistRange(60-70%)	2	94.33	100	100	91.67	100
12	DistRange(60-70%)_1 st diff.SG	2	96.99	100	100	100	100
13	DistRange(5-90%)_EtOHcomp	2	90.60	100	100	58.33	100
14	DistRange(60-70%)_1 st diff.SG_EtOHcomp	2	99.65	100	100	100	100

Model number, NC number of PCA principal components, %EV cumulative explained variance by NC principal components, **diff.SG** Savitzky-Golay derivative, **DistRange** Distillation Range used to build the model, **FullSpec** Complete NIRS measurement range, **SelSpec** Small more selective to ethanol signal, **EtOHcomp** component 2 related to ethanol.

Table 3 On-line batch MSPC results on test batches B10-23.

Test Batch	Method		
	Ind. Obs. ^a	FSMW ^b	Evolving ^c
on-spec			
B10	on-spec. ^d	on-spec.	on-spec.
B11	Q_{stat} .	on-spec.	on-spec.
off-spec			
B12	Q_{stat}, D_{stat} .	Q_{stat}, D_{stat} .	Q_{stat}, D_{stat} .
B13	Q_{stat}, D_{stat} .	Q_{stat}, D_{stat} .	Q_{stat}, D_{stat} .
B14	Q_{stat}, D_{stat} .	Q_{stat}, D_{stat} .	Q_{stat}, D_{stat} .
B15	Q_{stat}, D_{stat} .	Q_{stat}, D_{stat} .	Q_{stat}, D_{stat} .
B16	Q_{stat}, D_{stat} .	Q_{stat}, D_{stat} .	Q_{stat}, D_{stat} .
B17	Q_{stat}, D_{stat} .	Q_{stat}, D_{stat} .	Q_{stat} .
B18	Q_{stat}, D_{stat} .	Q_{stat}, D_{stat} .	Q_{stat} .
B19	Q_{stat}, D_{stat} .	Q_{stat}, D_{stat} .	Q_{stat} .
B20	Q_{stat}, D_{stat} .	Q_{stat}, D_{stat} .	Q_{stat} .
B21	Q_{stat}, D_{stat} .	Q_{stat}, D_{stat} .	Q_{stat} .
B22	Q_{stat}, D_{stat} .	Q_{stat}, D_{stat} .	Q_{stat} .
B23	Q_{stat}, D_{stat} .	Q_{stat}, D_{stat} .	Q_{stat} .

^a Ind.Obs., Individual observation MSPC models.

^b FSMW, fixed size moving window MSPC models.

^c Evolving MSPC models.

^d On-spec means the batch is on-specification according to both D_{stat} and Q_{stat} . D_{stat} means the batch is off-spec according to D_{stat} chart. Q_{stat} means the batch is off-spec. according to Q_{stat} chart.

9. List of Figures

Figure 1 Experimental setup of the automatic distillation device with on-line NIRS monitoring.

Figure 2 Process data from distillation batch B07. (a) Distillation curve, (b) On-line raw NIR spectra vs. percentage of the distilled fraction [wt%] and (c) raw NIR spectra at distilled fraction at 10, 50, 70 and 90 wt% indicated in (a), the spectra were vertically offsetted for clear comparison.

Figure 3 Plot of the (a) raw and (b) preprocessed NIR spectra obtained from the distillation batch B07 between 5 – 90 wt% with 1 wt% interval, 5 wt% (blue) → 90 wt% (red).

Figure 4 Different starting information used to build off-line PCA-based batch MSPC models (a) Distillation curves, (b) NIR information, from top to bottom: Original preprocessed NIR variables, concentration profiles from MCR-ALS and scores from PCA extracted from the multibatch structure for process modeling.

Figure 5 Different evolving on-line MSPC models approaches. a) Individual process observation models, b) Evolving MSPC models and c) FSMW-MSPC models.

Figure 6 Process modeling. (a) PCA map of the 3PC's scores from on-specification batches B01-09 used to build PCA model, and after projection in the PCA model batches B11 (on-specification) and B13 (off-specification). Start (5 wt%), transition region (60-70 wt%) and end (90 wt%) of distillation process are indicated; (b) Multibatch MCR-ALS showing from top to bottom the pure spectral profiles, the superimposed concentration profiles for on-specification batches B01-09 and concentration profiles for off-specification batch B13 (components (1) to (4)).

Figure 7 (a) Full distillation curves used to test PCA-based off-line batch MSPC model, on-specification in black and off-specification in gray, (b) $Dstat.$ and (c) $Qstat.$ MSPC charts. Some batches show higher $Dstat.$ and $Qstat.$ values and are not shown for better visualization of the control limits.

Figure 8 On-line MSPC charts for batches B11 (on-specification) and B18 (off-specification) for the a) Individual process observation models, b) Evolving MSPC strategies and c). FSMW evolving MSPC.

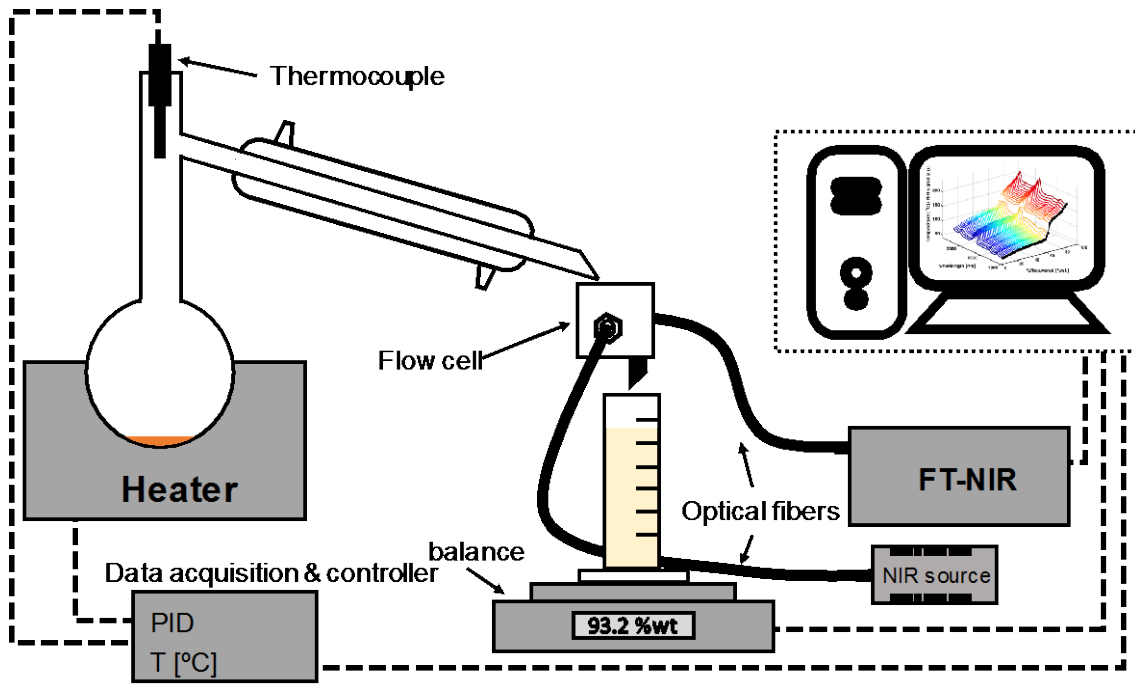


Figure 1 Experimental setup of the automatic distillation device with on-line NIRS monitoring.

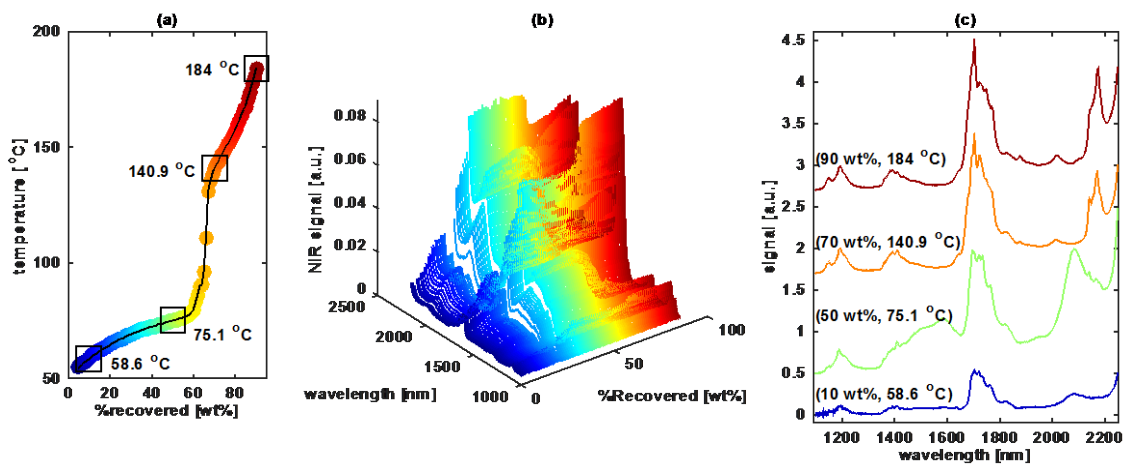


Figure 2 Process data from distillation batch B07. (a) Distillation curve, (b) On-line raw NIR spectra vs. percentage of the distilled fraction [wt%] and (c) raw NIR spectra at distilled fraction at 10, 50, 70 and 90 wt% indicated in (a), the spectra were vertically offsetted for clear comparison.

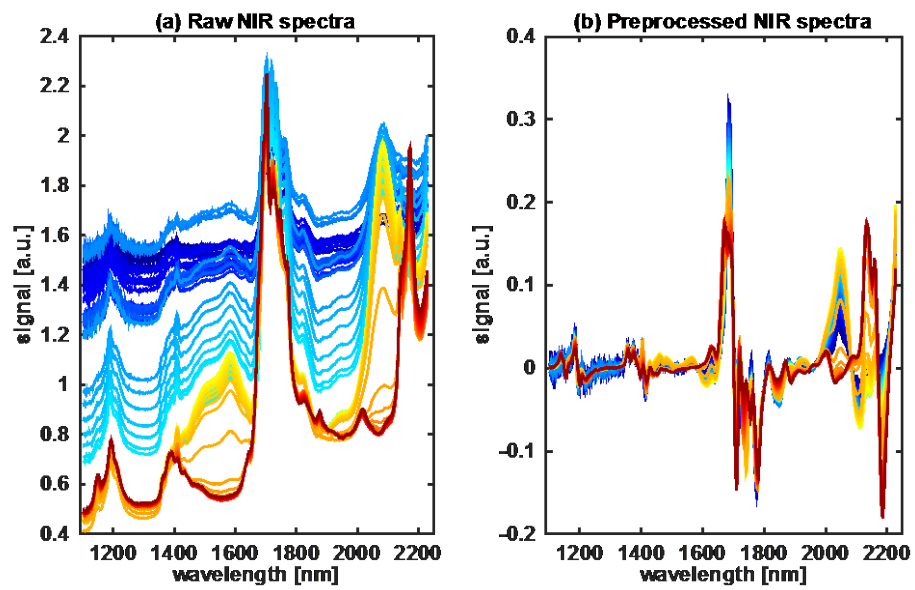
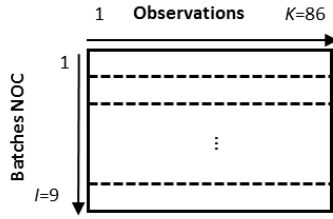


Figure 3 Plot of the (a) raw and (b) preprocessed NIR spectra obtained from the distillation batch B07 between 5 – 90 wt% with 1 wt% interval, 5 wt% (blue) → 90 wt% (red).

(a) Distillation Curves



(b) NIR information

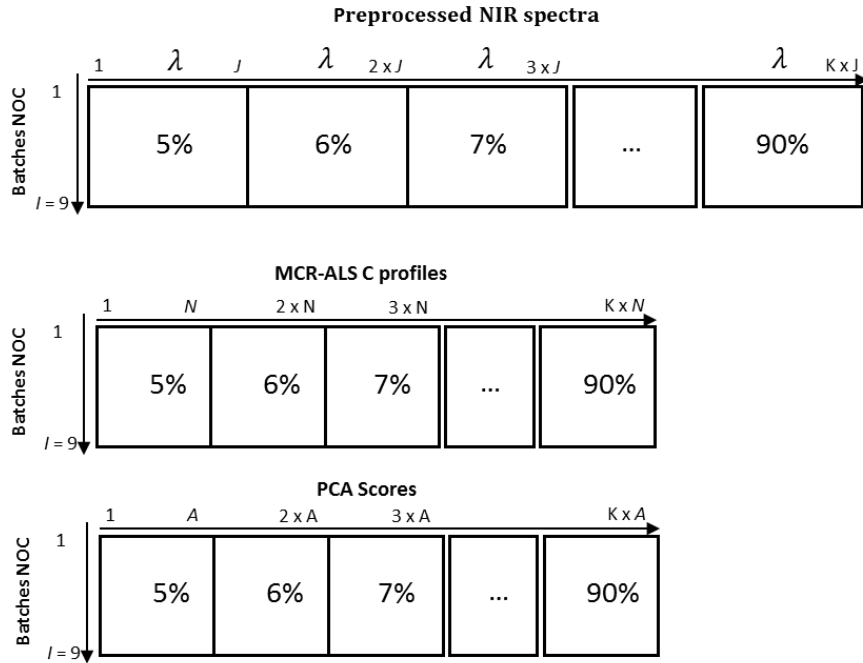


Figure 4 Different starting information used to build off-line PCA-based batch MSPC models (a) Distillation curves, (b) NIR information, from top to bottom: Original preprocessed NIR variables, concentration profiles from MCR-ALS and scores from PCA extracted from the multibatch structure for process modeling.

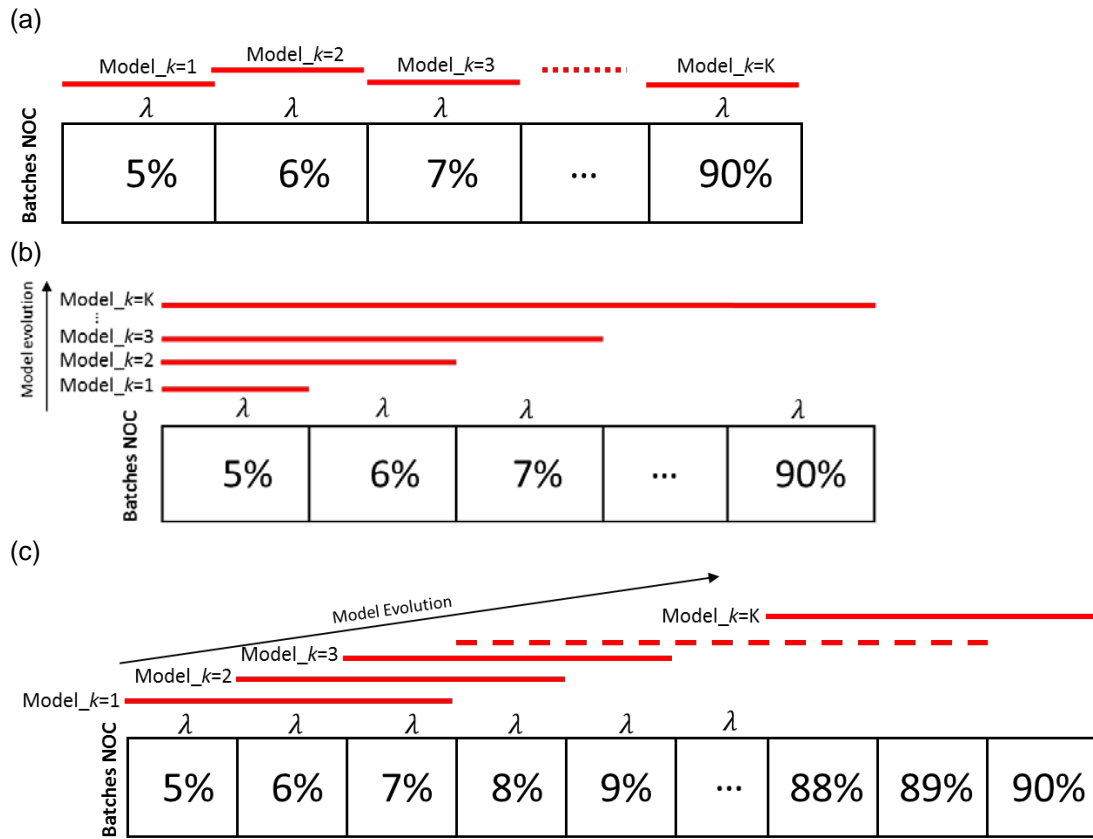


Figure 5 Different evolving on-line MSPC models approaches. a) Individual process observation models, b) Evolving MSPC models and c) FSMW-MSPC models.

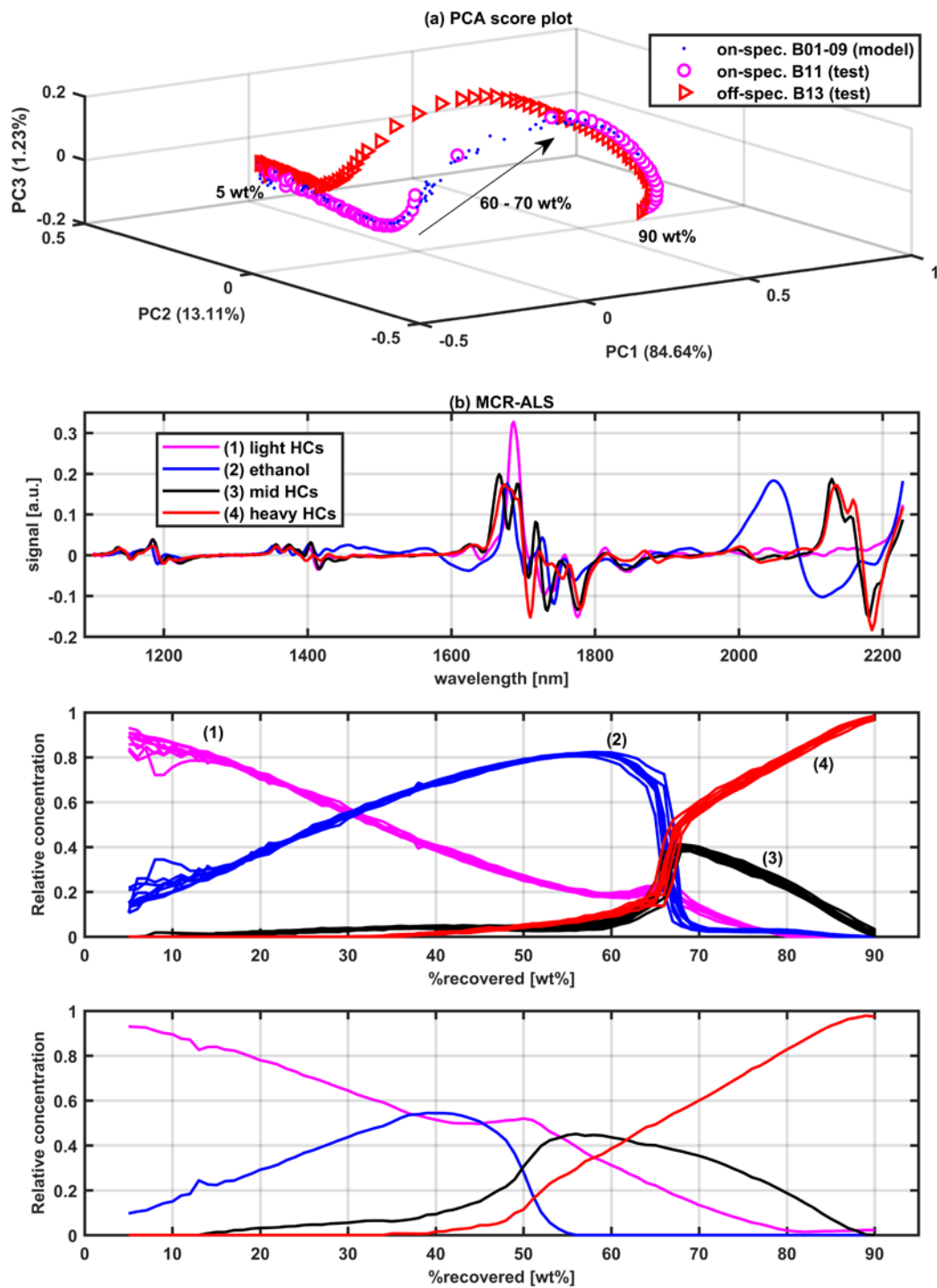


Figure 6 Process modeling. (a) PCA map of the 3PC's scores from on-specification batches B01-09 used to build PCA model, and after projection in the PCA model batches B11 (on-specification) and B13 (off-specification). Start (5 wt%), transition region (60-70 wt%) and end (90 wt%) of distillation process are indicated; (b) Multibatch MCR-ALS showing from top to bottom the pure spectral profiles, the superimposed concentration profiles for on-specification batches B01-09 and concentration profiles for off-specification batch B13 (components (1) to (4)).

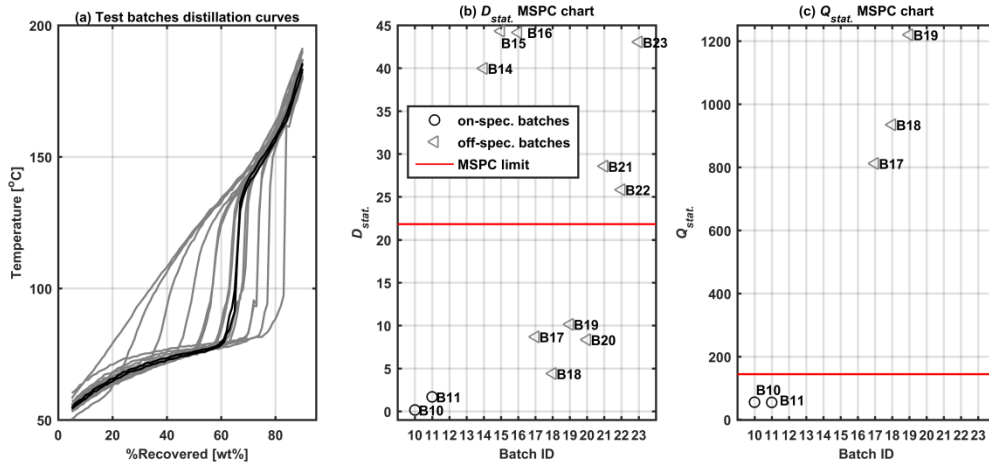


Figure 7 (a) Full distillation curves used to test PCA-based off-line batch MSPC model, on-specification in black and off-specification in gray, (b) $D_{stat.}$ and (c) $Q_{stat.}$ MSPC charts. Some batches show higher $D_{stat.}$ and $Q_{stat.}$ values and are not shown for better visualization of the control limits.

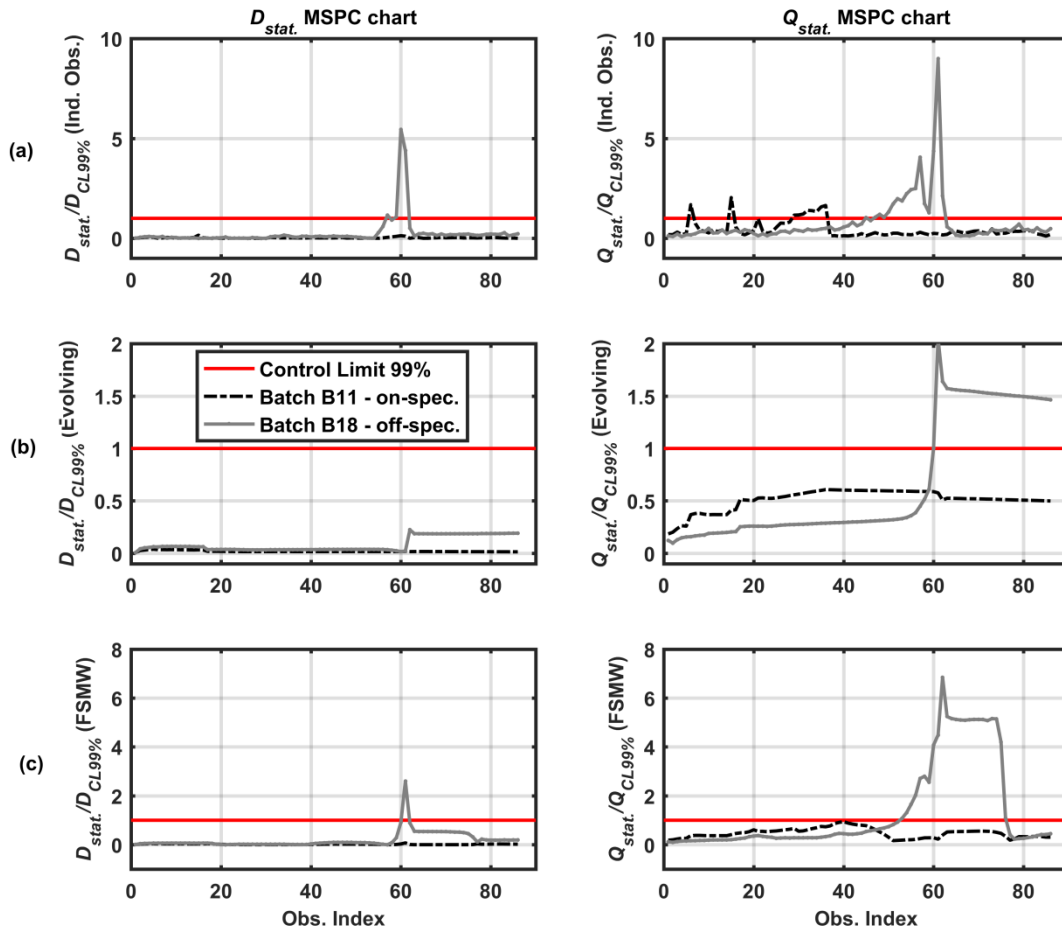


Figure 8 On-line MSPC charts for batches B11 (on-specification) and B18 (off-specification) for the a) Individual process observation models, b) Evolving MSPC strategies and c). FSMW evolving MSPC.